

Organic-Inorganic Hybrid Particles by Dendrimer Nanotemplating

Franziska Gröhn, Barry J. Bauer, Eric J. Amis

*Polymers Division, National Institute of Standards and Technology, Gaithersburg, Maryland
20899*

ABSTRACT

Poly(amidoamine) (PAMAM) dendrimers are used to create organic-inorganic hybrid colloids in aqueous solution. The formation of gold colloids upon reduction of a gold salt precursor serves as a model reaction to study the influence of reaction conditions and dendrimer generation on the resulting nanostructures. The hybrid particles were characterized by transmission electron microscopy (TEM), small angle neutron scattering (SANS), and small angle x-ray scattering (SAXS). A transition is found from “colloid stabilization” by low molecular mass molecules to “polymer nanotemplating” with increasing dendrimer generation, i.e., increasing molecular mass but retaining the chemical nature of the stabilizing species.

I. INTRODUCTION

Organic-inorganic hybrid nanostructures have generated significant interest due to a variety of potential applications as electrical, optical, medical and information storage materials. Biological nanocomposites like bone or sea shells produced in nature have excellent properties. The method of polymer nanotemplating, i.e., using a polymeric matrix to control the growth of an inorganic crystal, has been shown to be an effective synthetic route for producing polymer/inorganic composites[1]. However, the success of this approach requires understanding formation mechanisms and properties. Thus there is a need for model systems of polymer nanotemplating.

Since dendrimers are well defined organic molecules in the size range of (1 to 15) nm and are known to act as hosts for guest molecules [2,3], they are promising candidates as templates for the formation of inorganic nanoclusters. Organic-inorganic hybrid materials based on dendrimers have been recently reported by several authors [4-9]. However, our motivation for using dendrimers comes from a desire to understand the mechanisms of polymer nanotemplating in a model system. Dendrimers can serve a model system since they are monodisperse and well characterized molecules [10]. The size of different generation dendrimers spans the characteristic sizes of low molecular mass molecules, polymers and colloids, thereby offering a unique mesoscopic system.

In this study, we use charged polyamidoamine dendrimers in aqueous solution as potential nanotemplates. Our approach that is shown schematically in Figure 1 relies on the attraction between charged dendrimers and oppositely charged metal ions. Performing chemical reactions on the metal ions is expected to produce colloid structures that are controlled by the dendrimer. We use the reduction of gold salt to colloidal gold as a classical model reaction. The concept of using charged, solvent-penetrable templates in aqueous solution was first applied to polyelectrolyte microgels [11]. In this study, we investigate dendrimers from generation 2 to 10 (G2 to G10) for the formation of inorganic-organic hybrid colloids, whereas previous reports employed only low generation dendrimers (G6 and below). TEM, SANS and SAXS are employed to characterize the resulting organic-inorganic nanocomposites.

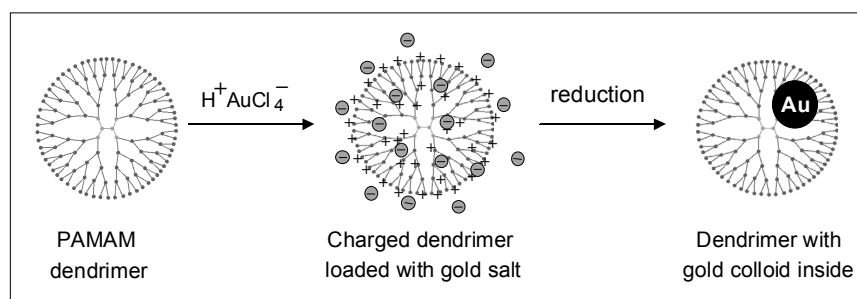


Figure 1. Dendrimer nanotemplating in aqueous solution. In a first step, the dendrimer is loaded with a precursor salt ($H^+AuCl_4^-$) resulting in a charged dendrimer with the precursor as counterions. In a second step, chemical reduction yields a colloid inside the dendrimer.

II. EXPERIMENTAL SECTION

Synthesis. PAMAM dendrimers of G2 to G4 were purchased from Aldrich Chemical Company and G5 to G10 were supplied by Dendritech (Michigan Molecular Institute) [12]. Dilute aqueous solutions of PAMAM dendrimers (mass fraction of 0.1 %) were mixed with aqueous solutions of $HAuCl_4$ at controlled stoichiometries. After stirring the solutions for 1 h, sodium borohydride in basic aqueous solution (0.1 mol/L NaOH) was added.

Transmission Electron Microscopy (TEM). Carbon coated copper grids, 300-mesh Formvar-free, were treated for (2 to 5) s in a glow-discharge tube to impart hydrophilic character to the carbon substrate. Stained specimens were prepared by depositing the sample solutions on the grid and inverting the grid on a drop of aqueous phosphotungstic acid solution (mass fraction of 2 %) that had been neutralized to pH = 7 with NaOH. The grid was then blotted on filter paper and air dried. TEM images were obtained at 120 kV with a Phillips 400 T at a magnification of 46000 X.

Small angle neutron scattering (SANS) Samples for SANS measurements were transferred into optical quality quartz banjo cells with 2 mm path length. SANS studies were performed at the Center for Neutron Research at the National Institute of Standards and Technology [13]. Measurements were made using the 30 m SANS instrument with a neutron wavelength $\lambda = 0.6$ nm and wavelength spread of $\Delta\lambda/\lambda = 0.15$. Data were corrected for empty quartz cell scattering, electronic background and detector uniformity, and converted to an absolute scale using secondary standards. The data were further corrected by subtracting the contributions from solvent scattering and incoherent background.

Small Angle X-ray Scattering (SAXS). SAXS data were collected at the Advanced Polymer Beamline at Brookhaven National Laboratory, X27C [14] using a 2D image plate detector (BAS2000, Fuji). The span of scattering vector magnitudes ($q = (4\pi/\lambda)\sin(\theta)$, 2θ scattering angle) was in the range $0.2 \text{ nm}^{-1} < q < 4.4 \text{ nm}^{-1}$. Experimental intensities were corrected for incident intensity and for background scattering. The scattering curves presented here were obtained by averaging three individual measurements. The uncertainties are the standard deviations of the mean intensity. All scattering intensities were corrected for solvent scattering. The scattering curve $I(q)$ was Fourier transformed into the pair distance distribution function $P(r)$ using the program ITP (*Indirect Transformation for the Calculation of $P(r)$*) by O. Glatter.[15,16,17]

III. RESULTS AND DISCUSSION

The nanotemplating by dendrimers in aqueous solution is depicted in Fig.1. The addition of HAuCl_4 to a neutral dendrimer with primary and tertiary amine groups results in a protonated dendrimer with AuCl_4^- counterions. The gold ions are reduced to metallic gold without the formation of a macroscopic metal precipitate. The stable brown to red solutions of colloidal gold formed indicate that the metal colloids were stabilized by the dendrimer. The stabilization of gold colloids in aqueous solution by the PAMAM dendrimers is possible over a wide range of reaction conditions. In order to control the size of the particles, one needs to optimize the ratio of the added gold ions to dendrimer, the dendrimer concentration in solution, as well as the reduction rate. Results reported here correspond to a loading ratio of dendrimer end groups to gold ions of 1:1, solutions with a dendrimer mass fraction of 0.12 % and a slow reduction rate (sodium borohydrate in basic solution).

TEM on G9-dendrimer-gold hybrid particles in Figure 2 indicates that the colloid particles are formed inside the dendrimer. One gold particle per dendrimer is predominantly formed.

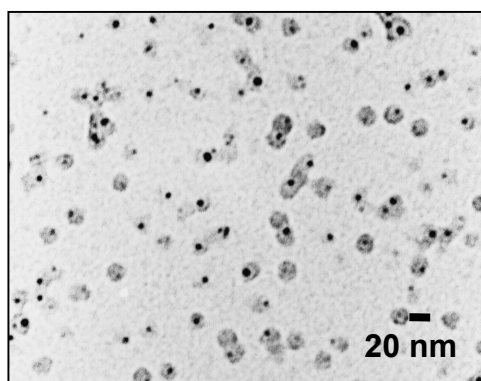


Figure 2. TEM of G9 PAMAM dendrimers containing gold colloids. The black dots are the gold and the 13 nm gray areas are the dendrimer stained with phosphotungstic acid.

SANS allows for the characterization of the dendrimer structure in solution. Measurements were performed on solutions of the unmodified dendrimer and the dendrimer-gold hybrid-particles in deuterium oxide. Guinier extrapolation of the scattering curves for the unmodified dendrimer and the gold containing dendrimers yields the same radius of gyration, showing that no aggregation of dendrimers takes place in solution.

SAXS provides more detailed information about the colloid structures. Figure 3 shows data for an unmodified G9 dendrimer, while Figure 4 for dendrimer-gold hybrid-particles. The different particle characteristics can be measured by Fourier transformation of the scattering curve $I(q)$ into real space, i.e. the pair distance distribution functions $P(r)$. The shape of $P(r)$ for the unmodified dendrimer shown in Figure 3b corresponds to a homogenous sphere of 13 nm diameter. In contrast, $P(r)$ for the hybrid particle in Figure 4b is typical of a layered sphere with a maximum dimension of 13 nm. These results prove that the gold is indeed formed inside of the dendrimer. Furthermore, modeling of the $P(r)$ reveals that the gold particle is located but offset from the dendrimer center. TEM and SAXS measurements of the gold particle diameter of 4 nm and dendrimer diameter of 13 nm are in agreement.

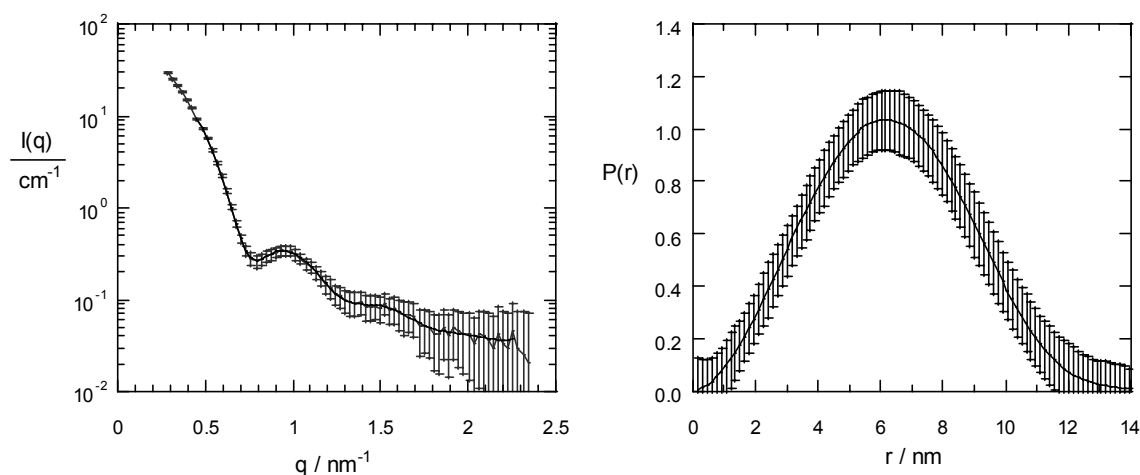


Figure 3. a) SAXS scattering curve, $I(q)$, for the unmodified G9 PAMAM-dendrimer. [18] and b) pair distribution function, $P(r)$, obtained by indirect Fourier transformation of the scattering data, $I(q)$.

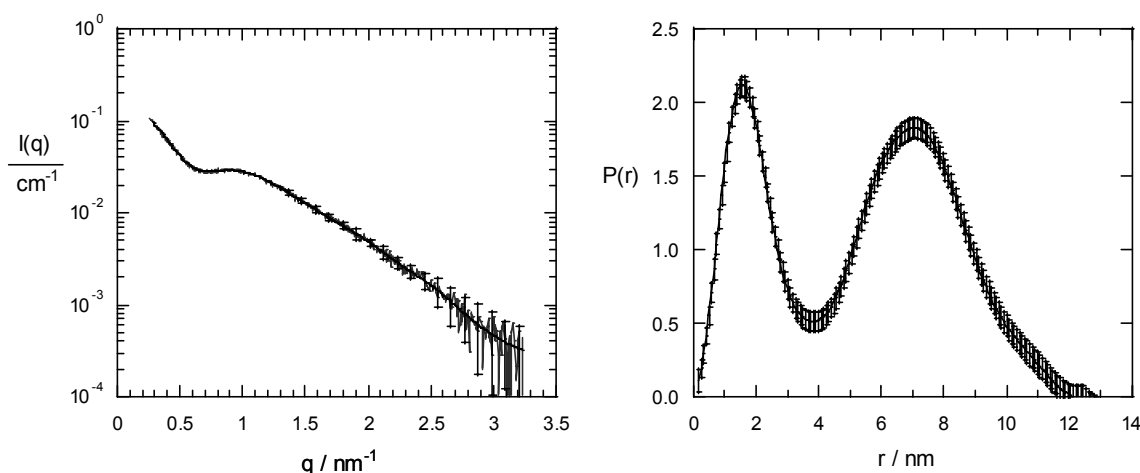


Figure 4. a) SAXS scattering curve, $I(q)$, for the gold containing G9 PAMAM-dendrimer [18] and b) pair distribution function, $P(r)$.

Thus, we have shown that the gold colloid is located inside the dendrimer and it is offset from the center as depicted schematically in Fig.1. The G9 dendrimer was loaded with gold salt corresponding to a gold-ion to end-group ratio of 1:1, which means 2048 gold ions per dendrimer molecule. Assuming the formation of one gold colloid from the loading of one dendrimer molecule upon reduction, one would expect a gold particle to consist of 2048 gold atoms. Based on this number, one expects a particle size of 4 nm, a calculated value that is in good agreement with the experimental results. Thus, we postulate that the gold ions from the loading of one dendrimer form one particle. The gold-colloid formation is indeed templated by the dendrimer. The ions added per dendrimer molecule form one particle. We will hereafter refer to this template mechanism as “fixed loading”.

It is of interest to investigate the effect of dendrimer generation on the size and structure of the hybrid particles formed. SAXS results for G7 to G10 are shown in Figure 5. For G7 to G9, individual dendrimer molecules containing single gold colloid particles are formed. The structure of the hybrid particles corresponds to the one of the G9 sample. The colloid diameters of 2.5 nm, 3.2 nm and 4 nm (within a range of ± 0.2 nm) agree well with the expected sizes for 512, 1024

and 2048 atoms. In contrast, for G10, multiple smaller gold particles inside one dendrimer are observed by TEM and SAXS.

In general, the growth of a colloid is determined by the free energy of the crystal formation and surface tension. When the colloid grows inside a polymeric matrix, the elastic forces of the surrounding polymer become important. The mass of the dendrimer molecule doubles with each generation, while the size increases only linearly, i.e., the internal dendrimer segment density increases slightly and the chain flexibility decreases. Conversely the volume of a single gold nanocluster would double with each generation. For the G10 dendrimer, it may be that the space available and the chain flexibility is not sufficiently high to allow for the growth of one colloidal particle. On the other hand, the increased surface to be stabilized for multiple smaller particles is likely to be provided by the G10 dendrimer. About four 3 nm gold colloids inside one G10 dendrimer are formed, which is in good agreement with the expected amount of 4096 atoms; thus the “fixed-loading” remains valid. Thus the G10 dendrimer realizes a host-guest nanotemplating, and the different dendrimer structure results in a different colloid morphology.

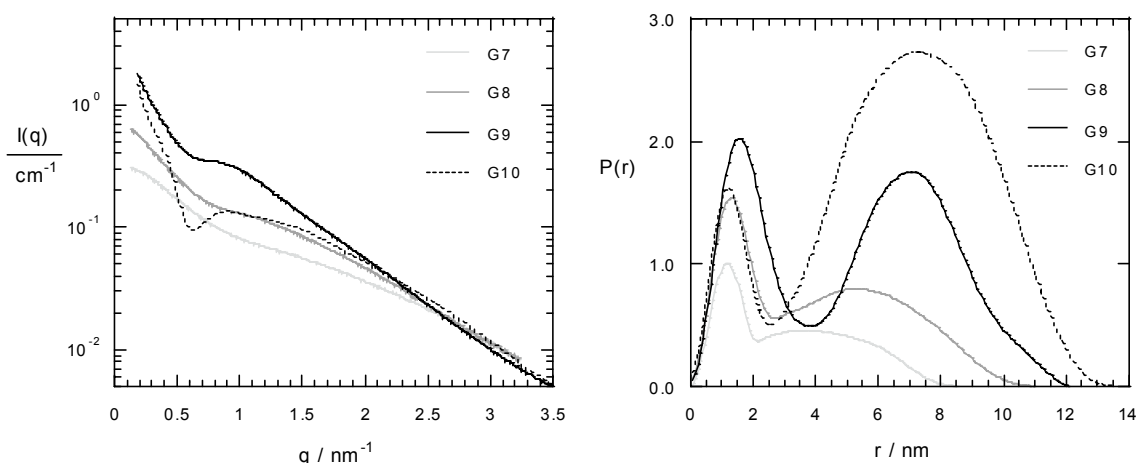


Figure 5. a) Small angle x-ray scattering curves $I(q)$ for gold-dendrimer hybrid structures obtained with PAMAM dendrimers of generation 7 to 10. [19] and b) Pair distribution functions, $P(r)$, obtained by indirect Fourier transformation of the scattering data, $I(q)$, in a). For G7 to G9 (solid lines) an increasing gold diameter with increasing dendrimer diameter is seen. However, for G10 (dotted line), the gold diameter is decreased although the dendrimer diameter is further increased. [20]

For G2 and G4 dendrimers, gold colloids of 4 nm and 2 nm diameter, respectively, are measured, both by TEM and SAXS, both being too large as to result from the gold ion load of one dendrimer. We also observe larger dendrimer aggregates. Thus, for low generation dendrimers the stabilizing mechanism is substantially different. The gold colloids are not formed inside a template, but multiple dendrimers become attached to the surface of one colloid when it is produced chemically. Again, one has to consider the structure of the dendrimer itself in order to understand this behavior. For the smallest dendrimers, a single dendrimer does not provide enough material to stabilize the surface of one gold colloid. In addition, very small metal clusters are less stable than large ones and therefore tend to form larger clusters containing the amount of gold from more than one dendrimer. This results in a hybrid structure of a metal colloid

surrounded by several dendrimers. The colloid stabilization can be considered as an analogue to the classical stabilization mechanism with low molar mass molecules. The molecules can become attached to the colloid surface and act as stabilizers, but they do not template the colloid.

IV. CONCLUSIONS

PAMAM dendrimers are shown to be effective as nanotemplates for inorganic nanocrystals. They not only stabilize the inorganic colloid in aqueous solution, but also determine the architecture of the nanostructures formed. G2 to G4 dendrimers behave like low molecular mass colloid stabilizers, i. e., several dendrimers become attached to the surface of the particle formed. G6 to G10 dendrimers act as effective “polymeric” templates. One colloid particle is formed inside one dendrimer, demonstrating a template mechanism known as “host-guest nanoscale synthesis”. To our knowledge, this is the first time such a transition has been shown from “colloid stabilization” by low molecular mass molecules to “polymer nanotemplating” with increase of molecular mass but constant chemistry of the stabilizing species.

Acknowledgements. This material is based upon work supported in part by the U.S. Army Research Office under contract number 35109-CH. We thank Donald Tomalia of MMI for providing us with dendrimers, Feng-Ji Yeh and Lizhi Liu for help with the SAXS setup, Paul Butler for help with the neutron scattering as well as Yvonne A. Akpalu, Catheryn L. Jackson and Brent D. Viers for helpful discussions.

REFERENCES

- [1] Antonietti, M.; Göltner, C.; *Angew. Chem Int. Eng. Ed.* **1997**, *36*, 910.
- [2] Jansen, J.F.G.A.; de Brabander-van den Berg, E.E.M.; Meijer, E.W.; *Science* **1994**, *266*, 1226.
- [3] Jansen, J.F.G.A.; Meijer, E.W.; *J. Am. Chem. Soc.* **1995**, *117*,4417.
- [4] Zhao, M.; Sun, L.; Crooks, R.M.; *J. Am. Chem. Soc.* **1998**, *120*,4877.
- [5] Sooklall, K.; Hanus, L.H.; *Advan. Mater.* **1998**, *10*, 1083.
- [6] Balogh, L.; Tomalia, D.A.; *J. Am. Chem. Soc.* **1998**, *120*, 7355.
- [7] Beck Tan, N.C.; Balogh, L.; Trevino, S.F.; *Polymer* **1999**, *40*, 2537.
- [8] Zhao, M.; Crooks, R.M.; *Adv. Mat.* **1999**,*11*,217.
- [9] Garcia, M.E.; Baker, L.A.; Crooks, R.M.; *Anal. Chem.* **1999**, *71*,256.
- [10] Prosa, T.J.; Bauer, B.J.; Amis, E.J.; Tomalia, D.A.; Scherrenberg, R.; *J. Polym. Sci.* **1997**, *35*, 2913.
- [11] Antonietti, M.; Gröhn, F.; Hartmann, J.; Bronstein, L.; *Angew. Chem Int. Eng. Ed.* **1997**, *36*, 2080.
- [12] Certain commercial materials and equipment are identified in this article in order to specify adequately the experimental procedure. In no case does such identification imply recommendation by the National Institute of Standards and Technology, nor does it imply that the material or equipment identified is necessarily the best available for this purpose.
- [13] Glinka, C.; Barker, J.G.; Hammouda, B.; Krueger, S.; Moyer, J.J.; Orts, W.J.; *J. Appl. Cryst.* **1998**, *31*, 430.
- [14] Hsiao, B.S.; Chu, B.; Yeh, F.; *NSLS Newsletter* **1997**, July1.
- [15] Glatter, O.; *Acta Phys. Austriaca* **1977**,*47*, 83.
- [16] Glatter, O.; *J. Appl. Cryst.* **1977**, *10*, 415.
- [17] Glatter, O.; *J. Appl. Cryst.* **1980**, *13*, 7 and 577.
- [18] Error bars are the measured standard deviation in I(q)
- [19] The relative standard deviation in the SAXS intensity values in the range $0.2 \text{ nm}^{-1} < q < 1.6 \text{ nm}^{-1}$ is less than 3 %. At higher wavevectors, the relative standard deviation increases with q to a maximum value of 7 %.
- [20] The relative standard deviation in the P(r) values is less than 3 %.